

Supporting Information

Facile preparation of bithiazole-based material for inkjet printed light-emitting electrochemical cell

Jingpei Huo*, Wanying Zou, Yubang Zhang, Weilan Chen, Xiaohong Hu, Qianjun Deng, and Dongchu Chen*

Institute of Electrochemical Corrosion, College of Materials Science and Energy Engineering, Foshan University, Foshan, 528000, P. R. China. Fax: 86-757-82966588; Tel: 86-757-82966588

*Corresponding Author E-mail:

johnhome222@163.com; cdcever@163.com;

Fax: 86-757-82966588; Tel: 86-757-82966588.

Experimental section

Materials and equipment

All reagents and solvents were commercially available and used as received.¹ Among them, rubeanic acid (99.0%) was purchased from TCI (Tokyo Chemical Industry Co., Ltd.). Hydroxyacetophenone (99%), iodomethane (CH₃I, AR), ethanol (AN, analytical grade) and acetic acid (HAc, AR) was purchased from Sinopharm Chemical Reagent Co., Ltd. (Shanghai, China). Copper(II) bromide (CuBr₂, 99%), 2'-hydroxyacetophenone (99%), *N*-bromosuccinimide (NBS, 99%), tetrakis(triphenylphosphine)palladium (Pd(PPh₃)₄, Pd ≥ 9.0%), sodium sulfate anhydrous (Na₂SO₄, 99.99%), sodium carbonate anhydrous (Na₂CO₃, 99.99%), cyclohexanone (≥ 99.5%) and tetrabutylammonium hexafluorophosphate (TBAPF₆, 98%) was purchased from Aladdin Co. Ltd. Pyren-4-ylboronic acid (PYR, 98%), 9-phenyl-9H-carbazol-3-ylboronic acid (CAR, 98%) and 9,9-dimethyl-9H-fluoren-3-ylboronic acid (FLUO, 98%) were purchased from Ruiyuan Group Limited (Yurui Chemical Co., Ltd.). Meanwhile, Nafion (5%) was purchased from J&K Chemical Ltd. Laboratory deionized (DI) water was achieved from an ultrapure water system, resulting in a resistivity >18 MΩ cm.

All the melting points were determined on a Yuhua X4 melting point apparatus (Gongyi, China) and were uncorrected. Infrared (IR) spectra were recorded on a Bruke Tensor 27 Fourier transform infrared (FT-IR) spectrometer by the KBr salt slice method in the absorption range of 4000-400 cm⁻¹. ¹H and ¹³C NMR spectra were obtained in DMSO-*d*₆ on a Bruker DRX-400 MHz spectrometer and tetramethylsilane (TMS) was used as internal standard. The mass spectra (MS) were recorded on Thermo LCQ DECA XP MAX mass spectrometer. Elemental analysis was performed on a Perkin Elmer Series II 2400 elemental analyzer.

The thermogravimetric analysis (TGA) was performed with TGA Q600 SDT TA Instruments apparatus (New Castle, DE, USA) at a heating rate of 10 °C/min under dry nitrogen (flow velocity 10 mL/min).

Steady-state UV-vis absorption measurements

UV absorption peaks were measured by Hitachi U-3010 absorption spectrophotometer with THF as solvent. And the corresponding samples were solved in THF to a 10 μ M concentration prior to the measurements, unless otherwise stated.²

Steady-state photoluminescence measurements

Photoluminescence (PL) spectra were measured by Hitachi F-4500 fluorescence spectrophotometer, with the excitation wavelength of 370 ± 5 nm. Moreover, the solid fluorescence quantum yields (ϕ_{PL}) values were determined employing a calibrated integrating sphere system ($\lambda_{exc} = 370 \pm 5$ nm).³

Photoluminescence lifetime measurements.

Time-resolved photoluminescence decay spectra were tested at room temperature with an Edinburgh FLS 920 Fluorescence spectrometer.

LECs Device fabrication and characterization

1.5*1.5 cm² indiumtin oxide (ITO, 20 ohms/square; Thin Film Devices, Anaheim, CA) with a thickness of 188 nm on a glass substrate were sequentially cleaned via acetone, methanol, isopropanol, and DI water in a sonicator, each for half an hour. Light-emitting electrochemical cells (LECs) were prepared by successively spin-coating ITO-coated glass substrates with poly(3,4-ethylenedioxythiophene)-poly(styrene sulfonate) (PEDOT-PSS, Aldrich; thickness: $d = 50$ nm) and active, material. The thickness of the active material was 100 nm. Consequently, a 150-nm Au top

contact (cathode) were deposited by thermal evaporation through a shadow mask at $p < 2 \times 10^{-4}$ Pa. The active area of each LEC device was 13 mm². All of the above device preparation procedures and measurements, were carried out in argon-filled glovebox ($[O_2] < 3$ ppm, $[H_2O] < 0.5$ ppm), except for washing the substrates and depositing PEDOT-PSS.⁶

Typical electroluminescence (EL) spectra and CIE coordinates were determined by a PR650 spectra colorimeter. The current-voltage and brightness-voltage curves of devices were measured using a Keithley 2400/2000 source meter and a calibrated silicon photodiode. All the measurements were carried out at room temperature under ambient conditions.⁷

Similar as for OLEDs, the external quantum efficiency (EQE) of LECs is expressed by **Eq. (4)**:

$$EQE = \gamma \eta_{s,t} q_{eff} \eta_{out} \quad (4)$$

γ is the charge balance coefficient, $\eta_{s,t}$ is the spin coefficient, q_{eff} is the effective radiative quantum factor and η_{out} is the out-coupling factor.⁸

Ink fabrication⁹⁻¹¹

The best performing ink formulation was subsequently used for the fabrication of a series of thin hybrid titania-silica film samples of variable thicknesses. Simple square 20 × 20 mm and 40 mm × 40 mm patterns were printed onto the microscopic and custom-cut glass substrates, respectively. Printing was repeated up to four times to obtain different overall thicknesses of titania-silica layers. Each layer was completely dried after printing so that the following layer was printed in the “wet-to-dry” manner. The deposition process was finalized by drying at 110 °C for 30 min to remove the high-boiling point components of the printing composition. Among them, the compound **1c** (15 mg*ml⁻¹) were separately dissolved in cyclohexanone in the mixture of PEO (10 mg ml⁻¹) under stirring at 50 °C. The active-material ink was stirred on a magnetic hot plate at 50 °C for >4 h before further processing. The

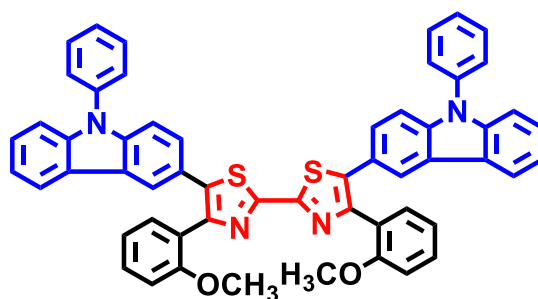
thickness of corresponding material was 105 nm, as measured with a stylus profilometer (Dektak XT, Bruker, US).

A 1 by 1 cm square patch was printed on one of the FTO strips created by scratching the FTO slides, thus forming the working photoanode, while the second strip remained naked for use as the counter electrode. Photoelectrodes of various thicknesses, with the thickest consisting of ten overprinted layers, were fabricated.

Synthesis

Starting from hydroxyacetophenone, CH₃I, rubeanic acid and PYR, CAR, FLUO as materials step by step, the bithiazole derivatives **1a-1c** was prepared according to the literature (Scheme S1).¹²⁻¹⁶

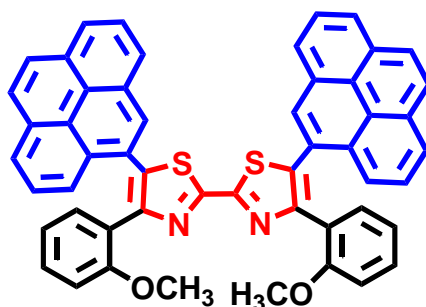
4,4'-bis(2-methoxyphenyl)-5,5'-bis(9-phenyl-9H-carbazol-3-yl)-2,2'-bithiazole (**1a**)



Yellow solid, yield 88%; UV-vis (CH₂Cl₂) λ_{\max} : 331 nm; ¹H NMR (400 MHz, DMSO-TMS) δ : 3.75 (s, 6H, 2CH₃), 7.31-7.38 (m, 2H, ArH), 7.41-7.50 (m, 8H, ArH), 7.52-7.61 (m, 8H, ArH), 7.64-7.71 (m, 6H, ArH), 7.70 (d, *J* = 8.0 Hz, 2H, ArH), 7.79 (d, *J* = 7.6 Hz, 2H, ArH), 8.01 (d, *J* = 8.0 Hz, 2H, ArH) ppm; ¹³C NMR (100 MHz, DMSO-TMS) δ : 56.94, 107.38, 111.53, 113.78, 116.88, 117.34, 119.13, 120.02, 120.89, 122.41, 123.34, 126.13, 127.24, 127.71, 129.29, 129.95, 130.75, 131.50,

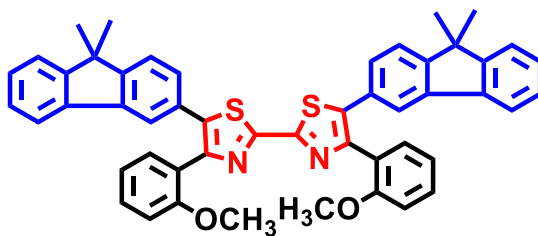
132.59, 137.49, 138.15, 140.51, 148.64, 153.82, 156.78, 158.31 ppm; IR (KBr) ν : 3073, 3062, 3040, 1690, 1640, 1591, 1539, 1493, 1348, 1234, 1194, 1071, 1025, 980, 741, 696 cm^{-1} ; ESI-MS, m/z (%): 885 ($[\text{M}+\text{Na}]^+$); Anal. Calcd for $\text{C}_{56}\text{H}_{38}\text{N}_4\text{O}_2\text{S}_2$: C 77.86, H 4.40, N 6.49, S 7.42; Found: C 77.79, H 4.46, N 6.53, S 7.51.

4-(2-methoxyphenyl)-2-(4-(2-methoxyphenyl)-5-(pyren-4-yl)thiazol-2-yl)-5-(pyren-4-yl)thiazole (1b)



pale green solid, yield 91%; UV-vis (CH_2Cl_2) λ_{max} : 328 nm; ^1H NMR (400 MHz, $\text{DMSO}-\text{TMS}$) δ : 3.77 (s, 6H, 2 CH_3), 7.06-7.15 (m, 14H, ArH), 7.17-7.21 (m, 2H, ArH), 7.27-7.37 (dd, $J_1 = J_2 = 8.0$ Hz, 6H, ArH), 7.60 (d, $J = 8.0$ Hz, 2H, ArH), 8.28 (d, $J = 8.0$ Hz, 2H, ArH) ppm; -- ^{13}C NMR (100 MHz, $\text{DMSO}-\text{TMS}$) δ : 57.86, 117.25, 119.75, 121.01, 123.80, 125.44, 126.63, 128.40, 128.87, 129.40, 130.19, 130.88, 131.28, 133.11, 135.64, 136.26, 139.08, 147.18, 148.01, 158.67, 159.43, 160.27 ppm; IR (KBr) ν : 3083, 3058, 3029, 1584, 1657, 1594, 1549, 1493, 1344, 1246, 1188, 1075, 1027, 972, 753.33, 694 cm^{-1} ; ESI-MS, m/z (%): 804 ($[\text{M}+\text{Na}]^+$, 100); Anal. Calcd for $\text{C}_{52}\text{H}_{32}\text{N}_2\text{O}_2\text{S}_2$: C 79.97, H 4.13 N 3.59, S 8.21; Found: C 79.88, H 4.52, N 3.45, S 8.32.

5,5'-bis(9,9-dimethyl-9H-fluoren-3-yl)-4,4'-bis(2-methoxyphenyl)-2,2'-bithiazole (1c)



Pale yellow solid, yield 86%; UV-vis (CH₂Cl₂) λ_{max} : 346 nm; ¹H NMR (400 MHz, DMSO-TMS) δ : 1.67 (s, 12H, 4CH₃), 3.87 (s, 6H, 2CH₃), 7.28-7.30 (m, 4H, ArH), 7.41-7.45 (m, 6H, ArH), 7.54-7.58 (m, 6H, ArH), 7.83 (d, *J* = 7.6 Hz, 2H, ArH), 7.95 (d, *J* = 8.0 Hz, 2H, ArH), 8.36 (d, *J* = 8.4 Hz, 2H, ArH) ppm; ¹³C NMR (100 MHz, DMSO-TMS) δ : 27.20, 46.89, 56.39, 118.54, 119.61, 120.22, 120.73, 122.35, 122.80, 127.09, 128.89, 129.48, 130.27, 130.93, 131.82, 132.33, 134.91, 138.84, 143.67, 153.02, 154.46, 156.95, 159.73, 161.85 ppm; IR (KBr) ν : 3082, 3060, 3036, 1693, 1658, 1572, 1522, 1491, 1355, 1233, 1157, 1073, 1025, 974, 784, 755 cm⁻¹; ESI-MS, *m/z* (%): 787 ([M+Na]⁺); Anal. Calcd for C₅₀H₄₀N₂O₂S₂: C 78.43, H 5.23, N 3.66, S 8.37; Found: C 78.50, H 5.29, N 3.62, S 8.28.

As an important reaction yielding aryl-aryl bonds, Suzuki coupling reaction, especially palladium catalyzed Suzuki coupling reaction is widely used in synthetic drugs, natural products, polymers and etc due to its many advantages, such as high yield, good regioselectivity, easy purification, convenient operation.^{17, 18} Hence, a series of novel bithiazole derivatives **1a-1c** were synthesized by the Suzuki coupling reaction between compound **4** and the respective heteroarylboronic acid in the presence of a palladium catalyst, with the isolated yields ranging from 86 to 91% (**Scheme S1**).

Their structures are characterized by IR, ¹H NMR, ¹³C NMR, MS, elemental analysis, UV-vis and photoluminescence (PL) spectroscopy, thermogravimetric analysis (TGA). Those relevant fluorescence dynamics, electroluminescence (EL) and electrochemical properties are measured. In the meantime, the donor groups and bithiazole-cores in the novel heterocyclic aromatic compounds **1a-1c** can make the π - π conjugate system longer, hoping to improve their thermal stability. Furthermore, these novel

bithiazole compounds **1a-1c** (**Figure S1**) symmetrically have some donor units, such as triarylamine, carbazole and fluorene, which will increase the electron density and effectively balance charge transport, making them steadier and improving their PL properties. The following discussions on the features reveal these luminescent materials are obtained indeed as expected.

The structures of the target compounds **1a-1c** are systematically characterized by UV, FTIR, ¹H NMR, ¹³C NMR, MS and elemental analysis. For example, in the UV spectra of the compounds **1a-1c**, there are strong absorption peaks in the region of 255-345 nm caused by $\pi \rightarrow \pi^*$ transition, which is from heterocyclic aromatic ring of donor groups. Moreover, there are strong absorption peaks in the region of 398-401 nm caused by $\pi \rightarrow \pi^*$ transition of the longer aromatic ring conjugate system in donor groups and thiazole moieties as expected.

In the IR spectra, the unsaturated C-H groups of aromatic rings show stretching absorption in the region of 3029-3083 cm^{-1} . At the same time, the strong C=N stretching band of thiazole rings appears at 1684-1695 cm^{-1} ,¹⁹ and the strongest C=C stretching band occurs in 1640-1678 cm^{-1} region. Besides, skeletal stretching vibrations of aromatic rings absorb in the region of 1484-1596 cm^{-1} . And the thiazole ring C-S stretching bands were observed around 1071-1088 cm^{-1} .^{20, 21}

When π -conjugated small molecules are applied to LECs fabrication, their thermal properties are usually examined by TGA. Meanwhile, (10% weight-loss temperature) is a standard for the thermal durability of these compounds.²² Those compounds have been checked by TGA measurements, the data are illustrated in **Figure S1** and summarized in **Table S1**.

In **Figure S1**, although they are heated to 250 °C, they can remain unchangeable, and they varied from 338 to 367 °C, indicating that all the compounds are high thermal stability. Moreover, both of the values for **1a** and **1b** were higher than 350 °C, while the one for **1c** was 338 °C. And the reason may be that both triphenylamine and carbazole contain no more than one aromatic group, which would remove

the alkyl groups in the side chain of electron-donating moiety and increase the crystallization characteristic, enhancing thermal stability.²² Hence, it can be concluded that they are thermally stable and suitable for LECs fabrication by vapor deposition.²³

Table S1. Physical properties of the compounds **1a-1c**

Compound	$T_{d_{10}}$ (°C)	$\lambda_{\max}^{\text{Abs}}$ (nm)	E_g^{opt} (eV)	E_{HOMO} (eV)	E_{LUMO} (eV)	$\lambda_{\max}^{\text{PL}}$ (nm)	ϕ_{PL}	τ (ns)
1	278	328	3.01	-4.93	-1.92	360	0.62	1.04,5.56
2	292	331	2.97	-4.91	-1.94	382	0.78	2.33,7.78
3	307	346	2.99	-4.95	-1.96	398	0.85	3.51,9.54

^aestimated from absorption onset of as-cast polymer film using the equation:

$$E_g^{\text{opt}} = 1240 / \lambda_{\text{onset}} \text{ (eV)}$$

$${}^b E_{\text{LUMO}} = -e(E_{\text{red}}^{\text{onset}} + 4.80) \text{ eV}$$

$${}^c E_{\text{HOMO}} = E_{\text{LUMO}} - E_g^{\text{opt}}$$

Table S2. Device properties with inkjet-printed vs. spin-coated emitter for **1c**.

Emitter	Properties				
	Bias (V)	Current Efficiency (Cd*A ⁻¹) _{max}	Efficiency (lm*W ⁻¹) _{max}	CIE 1931 coordinates (X, Y)	CRI
Inkjet-printed EML	3.3	16.02	9.80	(0.34, 0.43)	83
Spin-coated EML	3.1	11.84	6.92	(0.28, 0.42)	65

Table S3. LECs on the CIE chromaticity of standard blue color

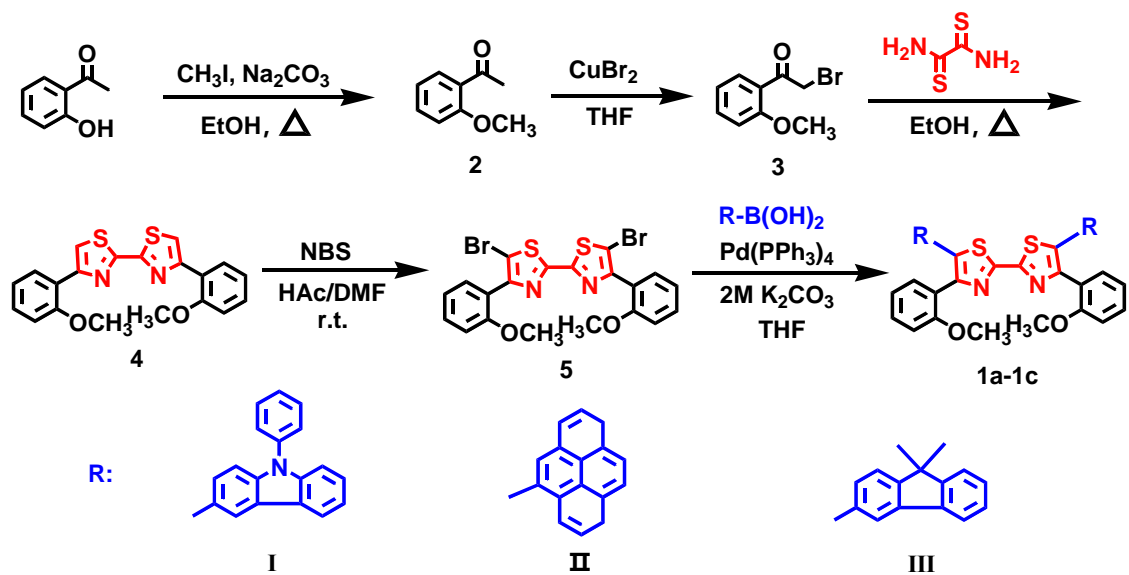
Emitter	$\lambda_{\text{max}}^{\text{Abs}}$ (nm)	Current efficiency (cd*A ⁻¹)	CIE 1931 coordinates (X, Y)	EQE (%)	Refs.
Cationic iridium complex	393	18.3	(0.17, 0.30)	18.9	[1]
Copper(I) complex	350	20	(0.23, 0.28)	Not reported	[2]
Naphthyl-linked phenanthroimidazole carbazole hybrid fluorophores	330	5.09	(0.153, 0.059)	6.96	[3]
Cationic polyfluorene	380	144	(0.26, 0.36)	0.05	[4]
Pyrene-imidazole derivatives	383	55	(0.17, 0.18)	Not reported	[5]
1c	398	35.12	(0.34, 0.43)	12.8	This work

References

- 1 K. Troshin and J. F. Hartwig, *Science*, 2017, **357**, 175.
- 2 J. Liu, J. Oliva, K. Tong, F. C. Zhao, D. Chen and Q. B. Pei, *Sci. Rep.*, 2017, **7**, 1524.

- 3 N. K. Metzger, R. Spesyvtsev, G. D. Bruce, B. Miller, G. T. Maker, G. Malcolm, M. Mazilu and K. Dholakia, *Nature Commun.*, 2017, **8**, 15610.
- 4 J. Park, J. Kim, J. Hong, H. Lee, Y. Lee, S. Cho, S.-W. Kim, J. J. Kim, S. Y. Kim and H. Ko, *NPG Asia Mater.*, 2018, **10**, 163.
- 5 M. Zhang, W. Gao, F. J. Zhang, Y. Mi, W. B. Wang, Q. S. An, J. Wang, X. L. Ma, J. L. Miao, Z. H. Hu, X. F. Liu, J. Zhang and C. L. Yang, *Energy Environ. Sci.*, 2018, **11**, 841.
- 6 S. Kim, H. J. Bae, S. Park, W. Kim, J. Kim, J. S. Kim, Y. Jung, S. Sul, S.-G. Ihn, C. Noh, S. Kim and Y. You, *Nature Commun.*, 2018, **9**, 1211.
- 7 L. Zhao, S. M. Wang, S. Y. Shao, J. Q. Ding, L. X. Wang, X. B. Jing and F. S. Wang, *J. Mater. Chem. C*, 2015, **3**, 8895.
- 8 S. Jenatsch, L. Wang, N. Leclaire, E. Hack, R. Steim, S. B. Anantharaman, J. Heier, B. Ruhstaller, L. Penninck, F. Nüesch and R. Hany, *Org. Electron.*, 2017, **48**, 77.
- 9 J. Zimmermann, L. Porcarelli, T. Rödlmeier, A. Sanchez-Sanchez, D. Mecerreyes, G. Hernandez-Sosa, *Adv. Funct. Mater.*, 2018, **28**, 1705795.
- 10 S. Jenatsch, M. Regnat, R. Hany, M. Diethelm, F. A. Nüesch and B. Ruhstaller, *ACS Photonics*, 2018, **5**, 1591.
- 11 J. Xu, A. Sandström, E. M. Lindh, W. Yang, S. Tang and L. Edman, *ACS Appl. Mater. Interfaces*, 2018, **10**, 33380.
- 12 J. P. Huo, Q. J. Deng, T. Fan, G. Z. He, X. H. Hu, X. X. Hong, H. Chen, S. H. Luo, Z. Y. Wang and D. C. Chen, *Polym. Chem.*, 2017, **8**, 7438.
- 13 J. P. Huo, H. W. Hu, M. Zhang, X. H. Hu, M. Chen, D. C. Chen, J. W. Liu, G. F. Xiao, Y. Z. Wang and Z. L. Wen, *RSC Adv.*, 2017, **7**, 2281.
- 14 J. P. Huo, H. W. Hu, G. Z. He, X. X. Hong, Z. H. Yang, S. H. Luo, X. F. Ye, Y. L. Li, Y. B. Zhang, M. Zhang, H. Chen, T. Fan, Y. B. Zhang, B. Y. Xiong, Z. Y. Wang, Z. B. Zhu and D. C. Chen, *Appl. Surf. Sci.*, 2017, **423**, 951.

- 15 J. P. Huo, Z. D. Hu, D. C. Chen, S. H. Luo, Z. Y. Wang, Y. H. Gao, M. Zhang and H. Chen, *ACS Omega*, 2017, **2**, 5557.
- 16 J. P. Huo and H. P. Zeng, *J. Mater. Chem. A*, 2015, **3**, 6258.
- 17 D. Perera, J. W. Tucker, S. Brahmabhatt, C. J. Helal, A. Chong, W. Farrell, P. Richardson and N. W. Sach, *Science*, 2018, **359**, 429.
- 18 E. L. Lucas and E. R. Jarvo, *Nature Rev. Chem.*, 2017, **1**, 65.
- 19 Z. Sahin, M. Ertas, B. Berk, S. N. Biltekin, L. Yurttas and S. Demirayak, *Bioorgan. Med. Chem.*, 2018, **26**, 1986.
- 20 J. M. Mašković, A. Hatzidimitriou, A. Damjanović, T. P. Stanojković, S. R. Trifunović, A. A. Geronikakie and D. Papagiannopoulou, *Med. Chem. Commun.*, 2018, **9**, 831.
- 21 A. A. Hassana, N. K. Mohamed, A. A. Aly, H. N. Tawfeek, S. Bräse and M. Nieger, *J. Mol. Struct.*, 2019, **1176**, 346.
- 22 S. Ameen, M. S. Akhtar, M. Nazim, M. K. Nazeeruddin and H.-S. Shin, *Nano Energy*, 2018, **49**, 372.
- 23 S. J. Yu, K. Pak, M. J. Kwak, M. Joo, B. J. Kim, M. S. Oh, J. Baek, H. Park, G. Choi, D. H. Kim, J. Choi, Y. Choi, J. Shin, H. Moon, E. Lee and S. G. Im, *Adv. Eng. Mater.*, 2018, **20**, 1700622.



Scheme S1. Synthesis of bithiazole-based compounds **1a-1c**

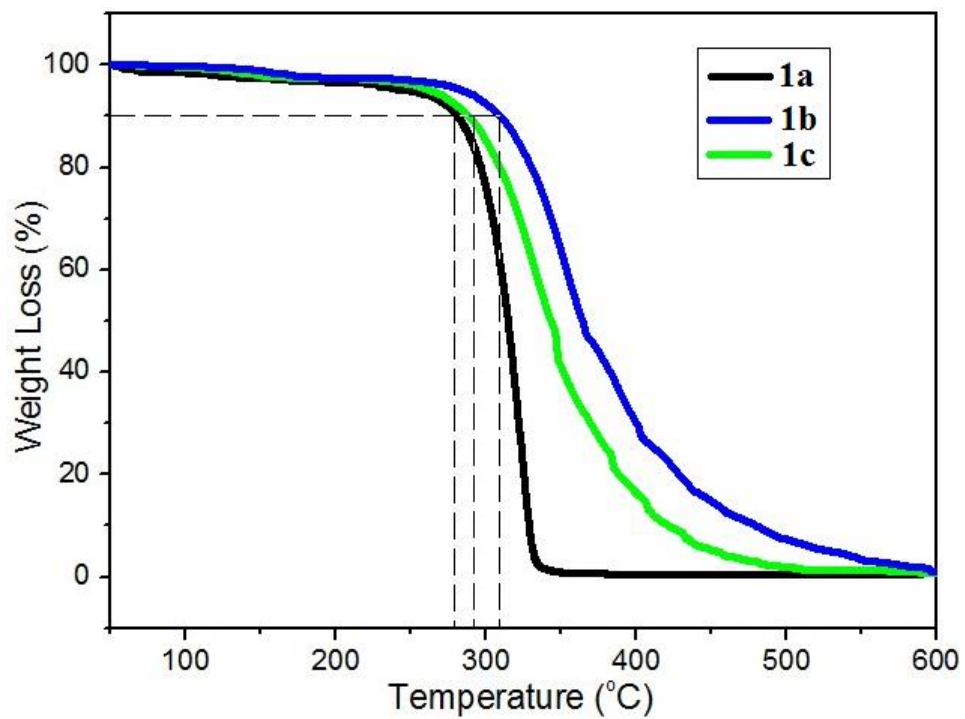


Figure S1 TGA traces recorded at a heating rate of $10\text{ }^{\circ}\text{C}\cdot\text{min}^{-1}$.

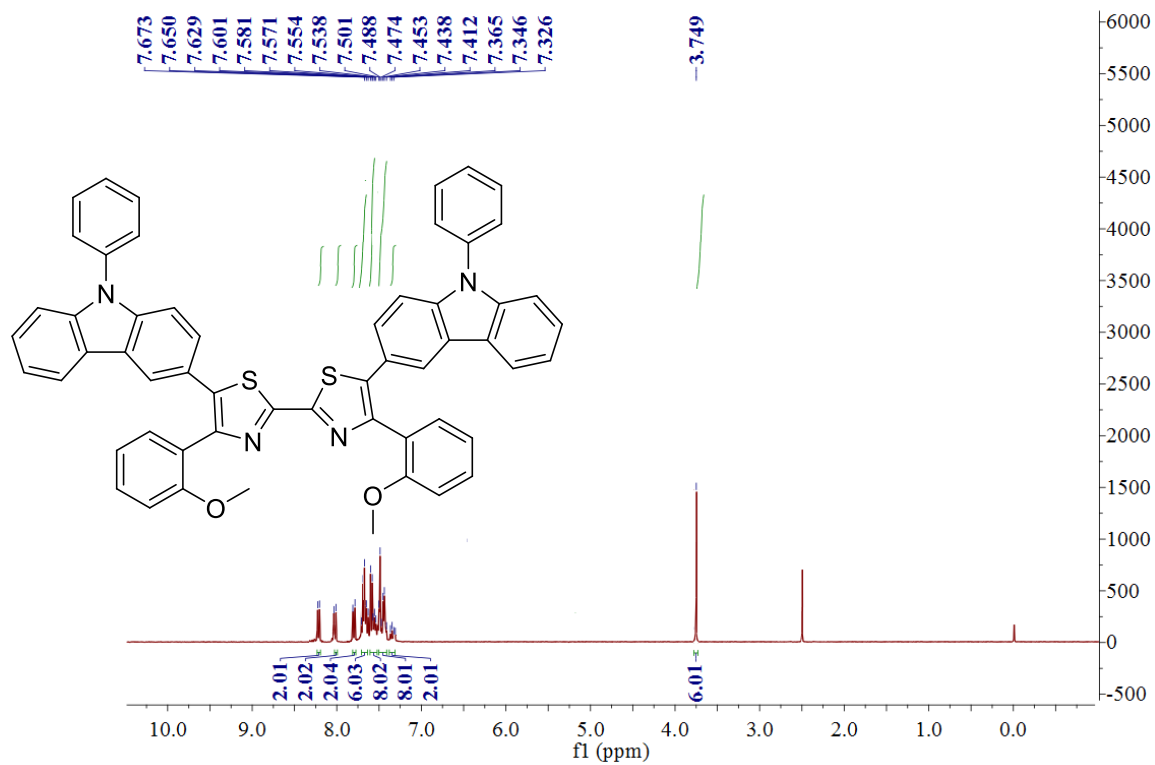


Figure S2. ¹H NMR spectrum of the compound **1a** in the *d*₆-DMSO.

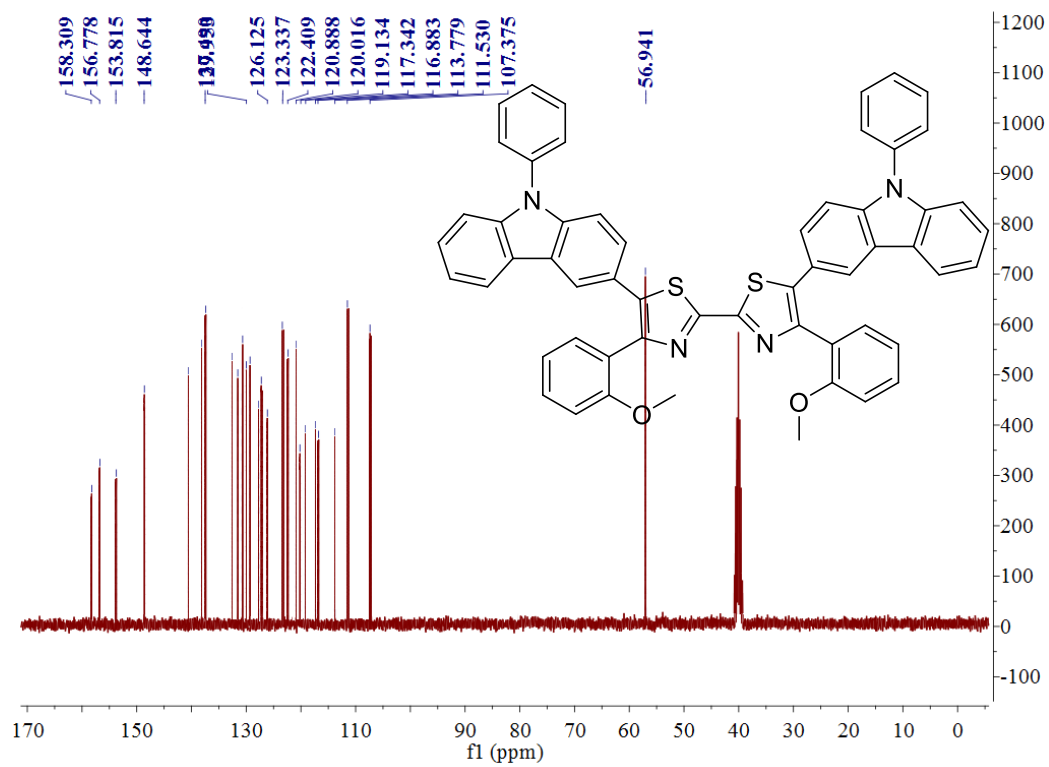


Figure S3. ^{12}C NMR spectrum of the compound **1a** in the d_6 -DMSO.

H10+ #12 RT: 0.14 A:1 NL: 1.19E7
T: + c ESI Full ms [500.00-1200.00]

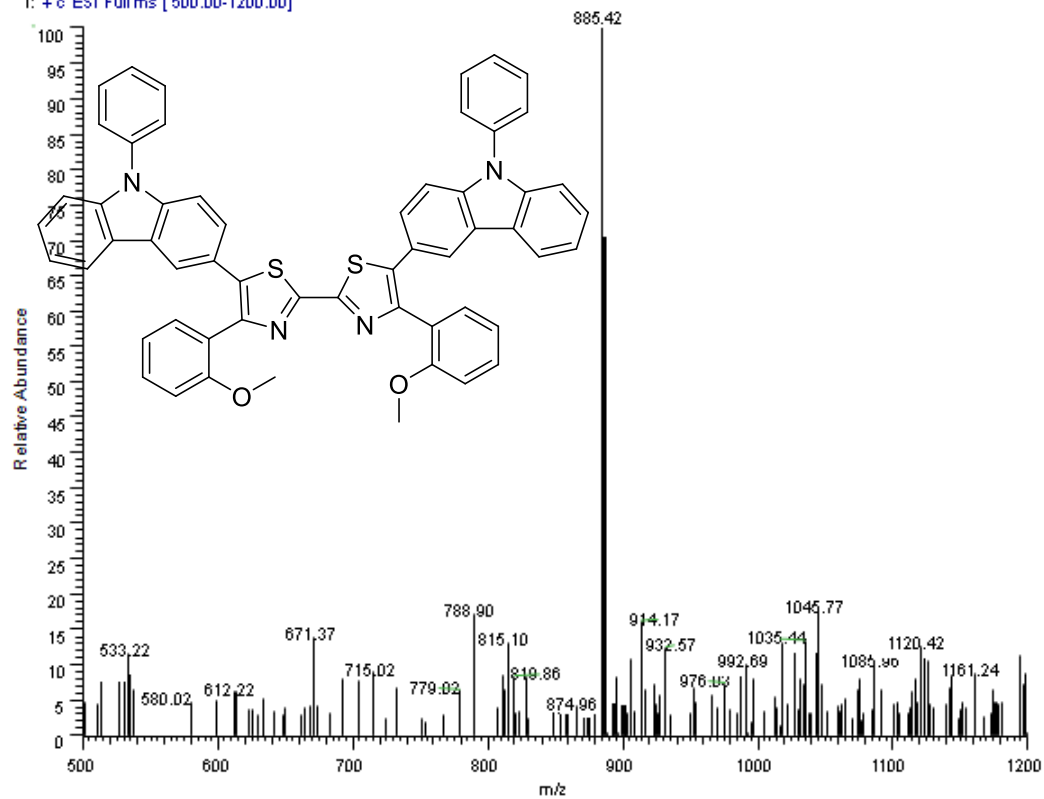


Figure S4. Mass spectrum of the compound **1a**.

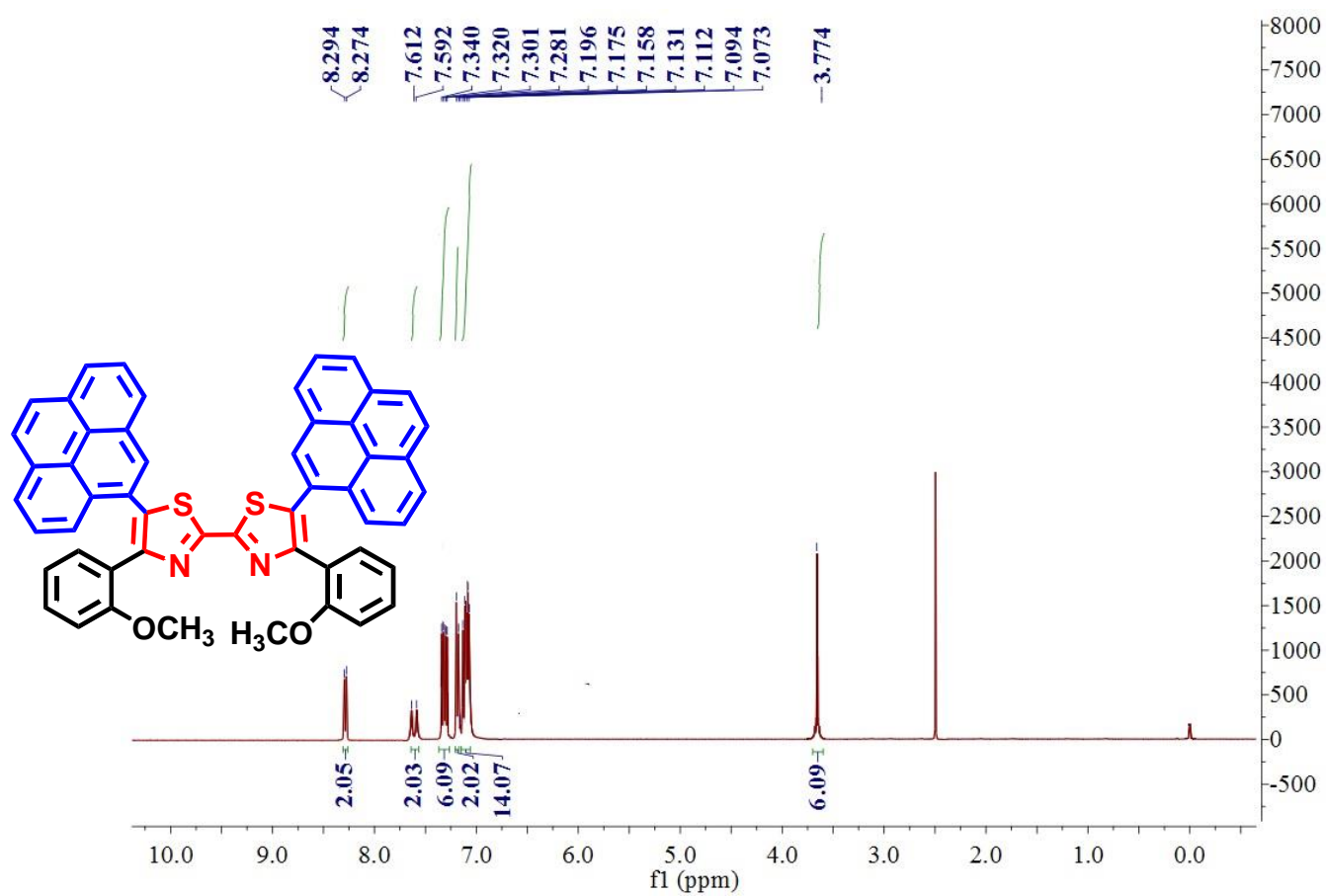


Figure S5. ¹H NMR spectrum of the compound **1b** in the *d*₆-DMSO.

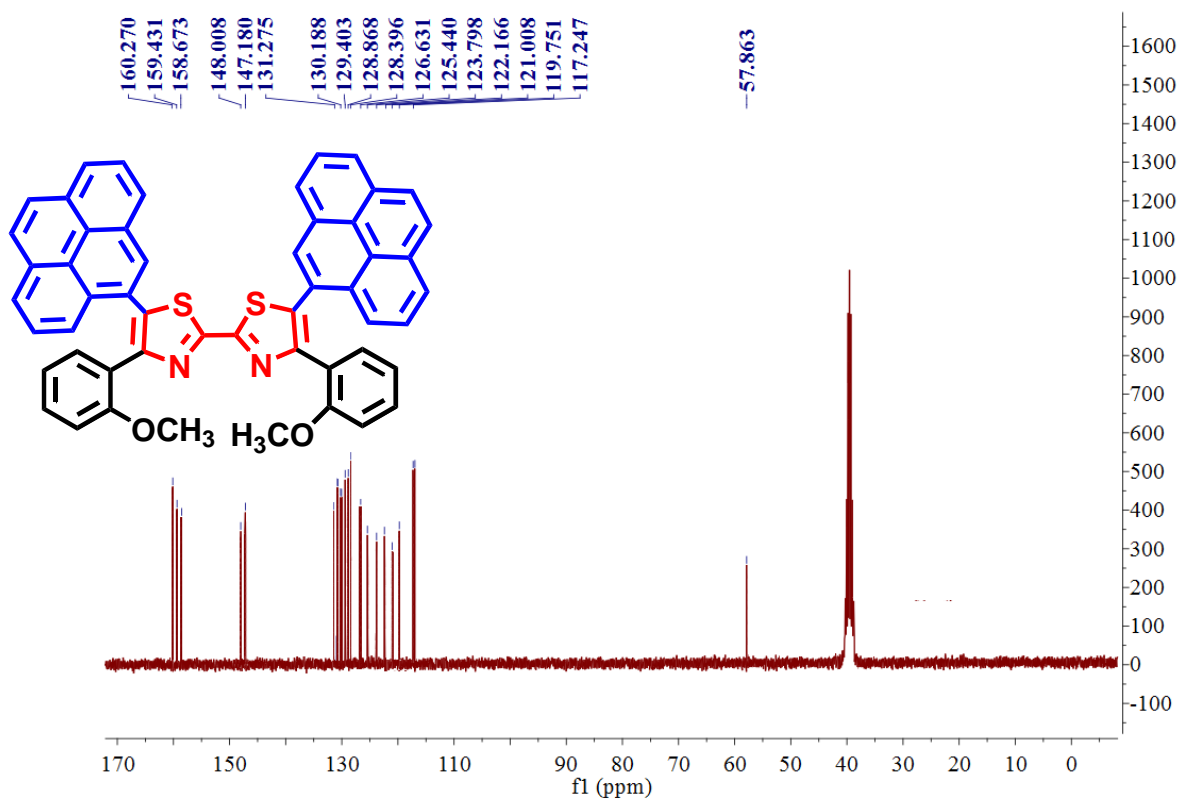


Figure S6. ^{12}C NMR spectrum of the compound **1b** in the d_6 -DMSO.

C2-2#13 RT: 0.14 A/L: 1 NL: 3.78E7
T: + c ESI Full ms [450.00-1200.00]

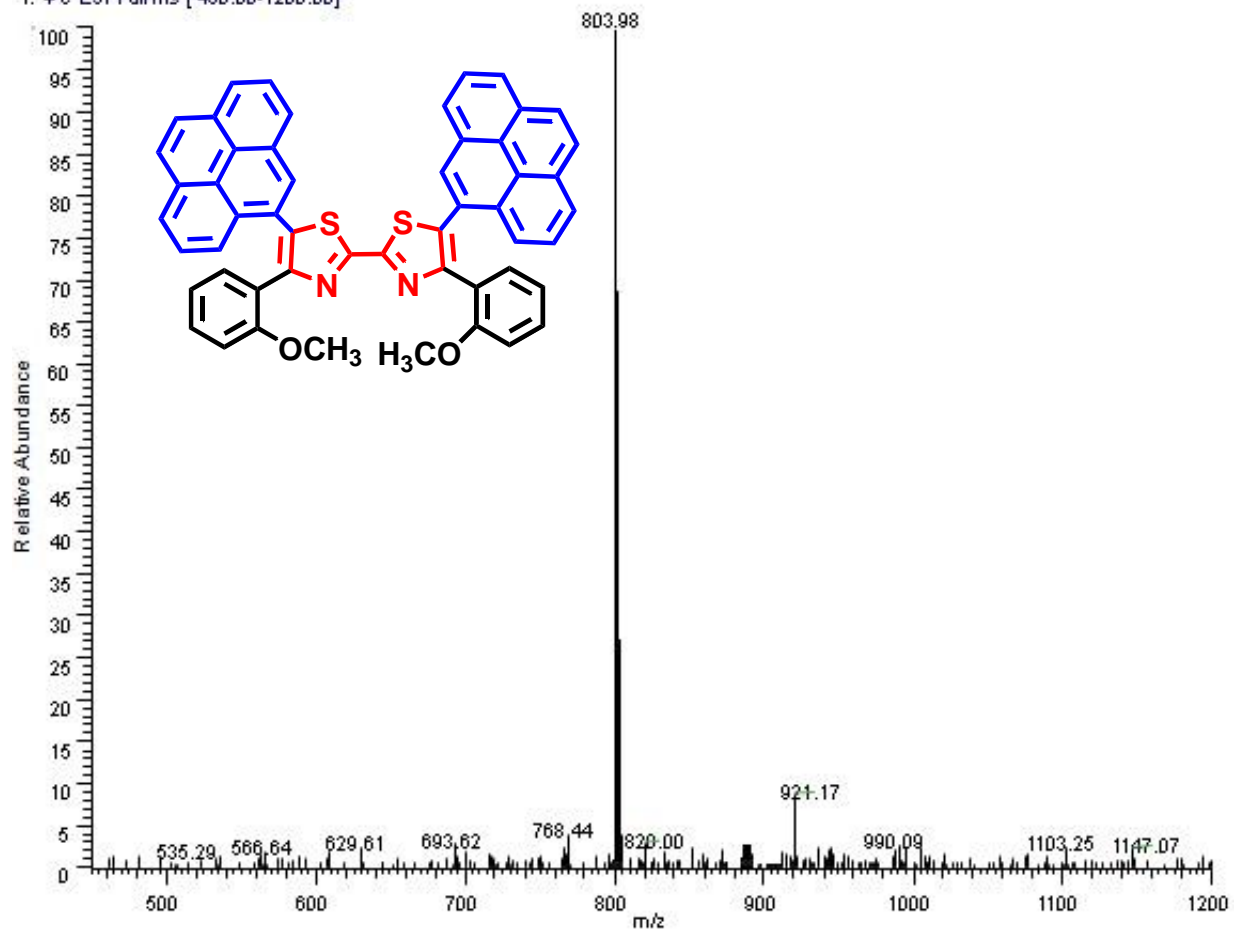


Figure S7. Mass spectrum of the compound **1b**.

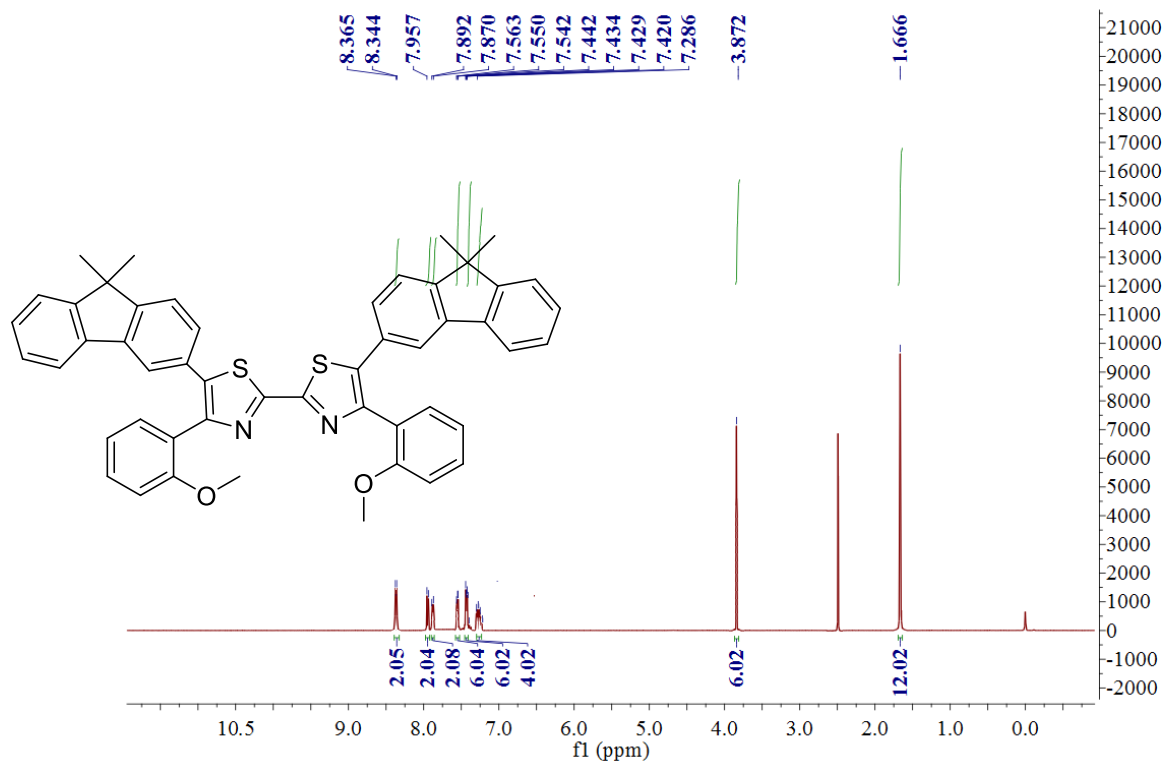


Figure S8. ¹H NMR spectrum of the compound **1c** in the *d*₆-DMSO.

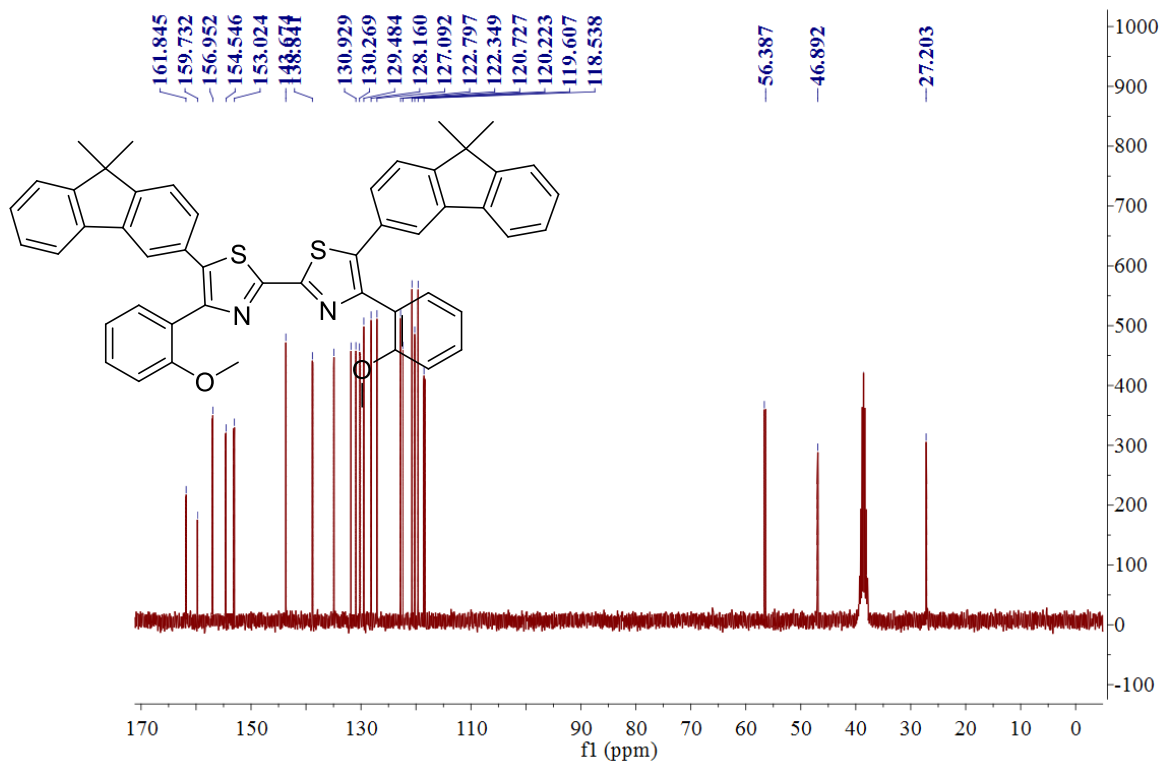


Figure S9. ¹³C NMR spectrum of the compound **1c** in the *d*₆-DMSO.

H10+ #12 RT: 0.14 A/L: 1 NL: 1.19E7
T: + c ESI Full ms [500.00-1200.00]

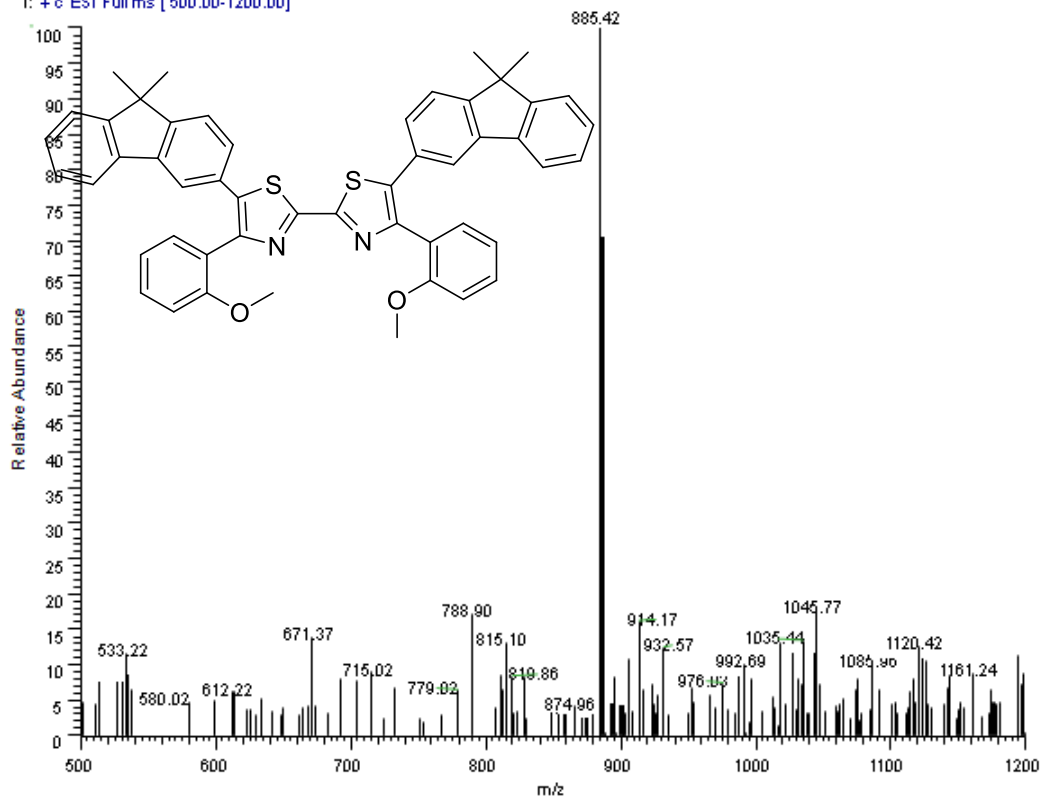


Figure S10. Mass spectrum of the compound 1c

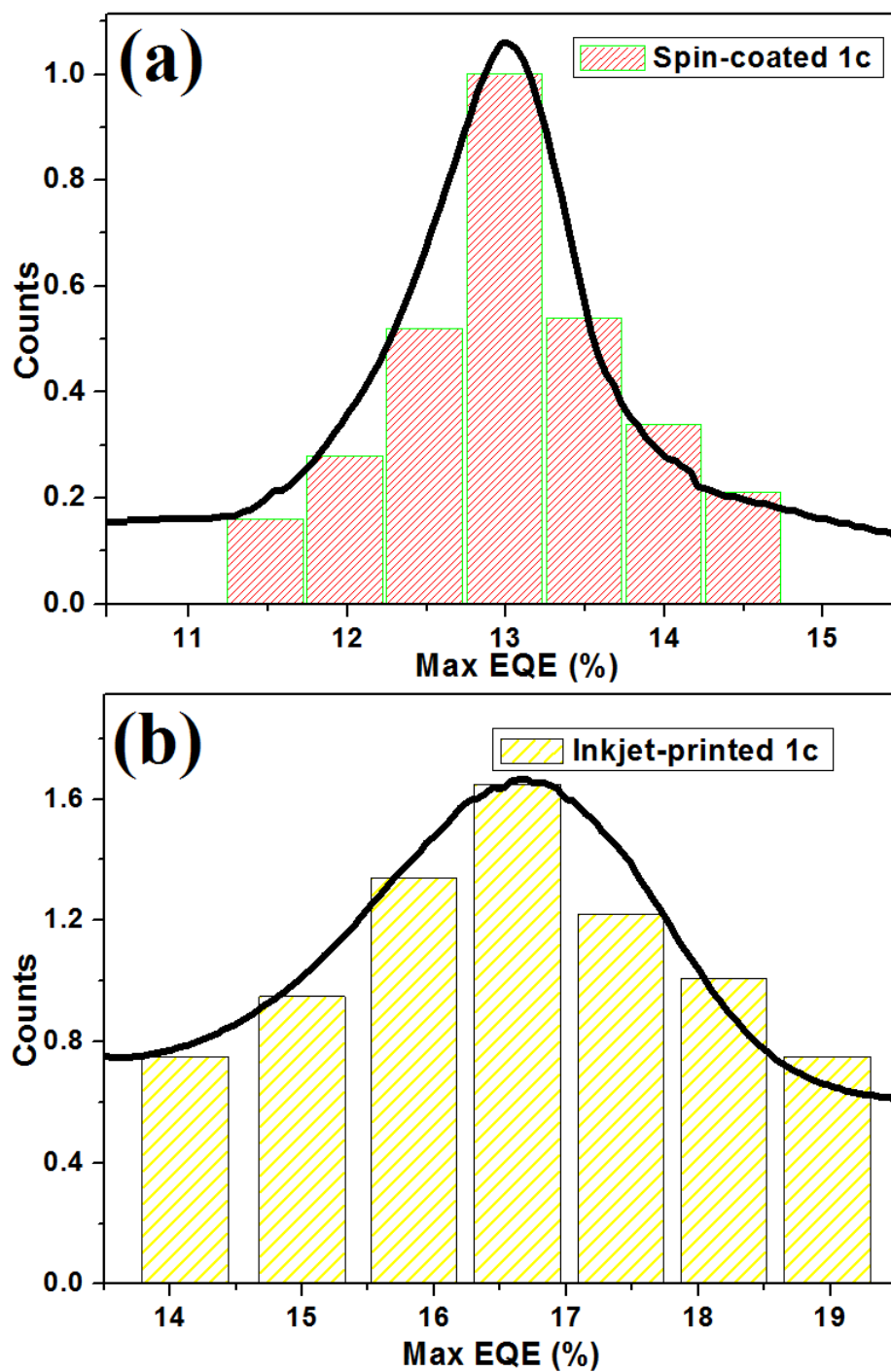


Figure S11. Histogram of the maximum EQEs of the unencapsulated LECs based on **1c**.